CHALMERS
FINITE ELEMENT CENTER

PREPRINT 2004–18

Adaptive Variational Multiscale Methods Based on A Posteriori Error Estimation: Energy Norm Estimates for Elliptic Problems

Mats G. Larson and Axel Målqvist

Chalmers Finite Element Center
CHALMERS UNIVERSITY OF TECHNOLOGY
Göteborg Sweden 2004

CHALMERS FINITE ELEMENT CENTER

Preprint 2004–18

Adaptive Variational Multiscale Methods Based on A Posteriori Error Estimation: Energy Norm Estimates for Elliptic Problems

Mats G. Larson and Axel Målqvist

CHALMERS

Chalmers Finite Element Center
Chalmers University of Technology
SE–412 96 Göteborg Sweden
Göteborg, October 2004

Adaptive Variational Multiscale Methods Based on A Posteriori Error Estimation: Energy Norm Estimates for Elliptic Problems
Mats G. Larson and Axel Målqvist
NO 2004–18
ISSN 1404–4382

Chalmers Finite Element Center
Chalmers University of Technology
SE–412 96 Göteborg
Sweden
Telephone: +46 (0)31 772 1000
Fax: +46 (0)31 772 3595
www.phi.chalmers.se

Printed in Sweden
Chalmers University of Technology
Göteborg, Sweden 2004

Adaptive Variational Multiscale Methods Based on A Posteriori Error Estimation: Energy Norm Estimates for Elliptic Problems

Mats G. Larson * Axel Målqvist †

October 8, 2004

Abstract

The variational multiscale method provides a framework for construction of adaptive multiscale finite element methods. We develop a new adaptive finite element method based on the variational multiscale method and we derive an a posteriori error estimate in energy norm. The estimate captures crucial parameters of the method and shows how they are related. We present an adaptive algorithm that tunes these parameters automatically according to the a posteriori error estimate. Finally, we show how the method works in practice by presenting various numerical examples.

1 Introduction

The application of multiscale problems are numerous. They appear in all branches of the engineering sciences e.g. composites materials, flow in porous media, fluid mechanics, and quantum physics. A common feature for all these applications is that they are very computationally challenging and often impossible to solve to an acceptable tolerance with standard one mesh methods. New methods needs to be found and together with new method we need new error estimates to ensure the accuracy of the methods.

Previous work. The Variational Multiscale Method (VMM) serves as a general framework for the solution of multiscale problems, see [7, 9]. The idea is to decompose the solution into fine and coarse scale contributions, solve fine scale equation in terms of the

*Corresponding author, Department of Computational Mathematics, Chalmers University of Technology, Göteborg, S-412 96, Sweden, mgl@math.chalmers.se

†Department Computational Mathematics, Chalmers University of Technology, Göteborg, S-412 96, Sweden, axel@math.chalmers.se

coarse scale residual, and finally eliminate the fine scale solution from the coarse scale equation. This procedure leads to a modified coarse scale equation where the modification accounts for the effect of fine scale behavior on the coarse scales. In several works various ways of analytical modeling are investigated often based on bubbles or element Green's functions, see Hughes [7], Oberai and Pinsky, [12], and Arbogast [1]. In [6] Hou and Wu present a different approach. Here the fine scale equations are solved numerically on a finer mesh. The fine scale equations are solved inside coarse elements and are thus totally decoupled.

In the adaptive variational multiscale method (AVMM), introduced in [11, 10] the fine scale equations are decoupled and solved approximately on patches. In [10] an error estimate is presented for control of a linear functional of the error. The method is adaptive in the sense that both the areas where local problems are solved and the accuracy of the solution of the local problems are chosen automatically.

New contributions. The focus of this paper is to present an a posteriori error estimate of AVMM in the energy norm. The basic idea of AVMM is to split the fine scale residual into localized contributions using a partition of unity and solving corresponding decoupled localized problems on patches with homogeneous Dirichlet boundary conditions. The fine scale solution is approximated by the sum $U_f = \sum_i U_{f,i}$ of the solutions $U_{f,i}$ to the localized problems associated with coarse node i. The accuracy of U_f depends on the fine scale mesh size h and the size of the patches. We note that the fine scale computation is naturally parallel.

To optimize performance we want to construct an adaptive algorithm for automatic control of the coarse mesh size H, the fine mesh size h, and the size of patches. The algorithm is based on the following a posteriori estimate of the error $e = u - U_c - U_f$ in the energy norm for the Poisson equation with variable coefficient a:

$$\begin{aligned} \|e\|_a^2 \leq C \sum_{i \in \mathcal{C}} \|H\mathcal{R}(U_c)\|_{\omega_i}^2 \|\frac{1}{\sqrt{a}}\|_{L^\infty(\omega_i)}^2 \\ + C \sum_{i \in \mathcal{F}} \left(\|\sqrt{H}\Sigma(U_{f,i})\|_{\partial\omega_i}^2 + \|h\mathcal{R}_i(U_{f,i})\|_{\omega_i}^2 \right) \|\frac{1}{\sqrt{a}}\|_{L^\infty(\omega_i)}^2, \end{aligned} \tag{1.1}$$

where

$$(-\Sigma(U_{f,i}), v_f)_{\partial\omega_i} = (f + \nabla \cdot a\nabla U_c, \varphi_i v_f)_{\omega_i} - a(U_{f,i}, v_f)_{\omega_i}, \ \text{ for all } v_f \in V_f^h(\bar{\omega}_i), \tag{1.2}$$

$\mathcal{C}$ refers to nodes where no local problems have been solved, $\mathcal{F}$ to nodes where local problems are solved, U_c is the coarse scale solution, $U = U_c + U_f$, $\{\varphi_i\}_{i \in \mathcal{C} \cup \mathcal{F}}$ is a partition of unity, $\mathcal{R}(U)$ is a computable bound of the residual $f + \nabla \cdot a\nabla U$, $\mathcal{R}_i(U_{f,i})$ is a bound of the fine scale residual $\varphi_i(f + \nabla \cdot a\nabla U_c) + \nabla \cdot a\nabla U_{f,i}$, $\Sigma(U_{f,i})$ is related to the normal derivative of the fine scale solution $U_{f,i}$ and measures the effect of restriction to patches. If no fine scale equations are solved we obtain the first term in the estimate; the first part of the second sum measures the effect of restriction to patches; and finally the second part measures the influence of the fine scale mesh parameter h.

The framework of AVMM is fairly general and may be extended to other types of multiscale methods, for instance, based on localized Neumann problems.

Outline. In Section 2 we introduce the model problem and the adaptive variational multiscale formulation. In Section 3 we present a posteriori error estimates. We study the special case of periodic coefficient in Section 4 and present an adaptive algorithm based on the error analysis in Section 5. Finally, in section Section 6 we present numerical results.

2 The Variational Multiscale Method

2.1 Model Problem

We study the Poisson equation with a coefficient a and homogeneous Dirichlet boundary conditions: find $u \in H^1_0(\Omega)$ such that

$$-\nabla \cdot a\nabla u = f \quad \text{in } \Omega, \tag{2.1}$$

where Ω is a polygonal domain in $\mathbf{R}^d$, $d = 1, 2$, or 3 with boundary Γ, $f \in L^2(\Omega)$, and $a \in L^\infty(\Omega)$ such that $a(x) > 0$ for all $x \in \Omega$. The variational form of (2.1) reads: find $u \in \mathcal{V} = H^1_0(\Omega)$ such that

$$a(u, v) = (f, v) \quad \text{for all } v \in \mathcal{V}, \tag{2.2}$$

with the bilinear form

$$a(u, v) = (a\nabla u, \nabla v), \tag{2.3}$$

for all $u, v \in \mathcal{V}$.

2.2 The Variational Multiscale Method

We focus on two scales and employ the variational multiscale scale formulation, proposed by Hughes see [7, 9] for an overview. We choose two spaces $\mathcal{V}_c \subset \mathcal{V}$ and $\mathcal{V}_f \subset \mathcal{V}$ such that

$$\mathcal{V} = \mathcal{V}_c \oplus \mathcal{V}_f, \tag{2.4}$$

where $\mathcal{V}_c$ is associated with the coarse scale and $\mathcal{V}_f$ is associated with the fine scale. Introducing these spaces in (2.2) gives us the following weak formulation: find $u_c \in \mathcal{V}_c$ and $u_f \in \mathcal{V}_f$ such that

$$\begin{aligned} a(u_c, v_c) + a(u_f, v_c) &= (f, v_c) \quad \text{for all } v_c \in \mathcal{V}_c, \\ a(u_c, v_f) + a(u_f, v_f) &= (f, v_f) \quad \text{for all } v_f \in \mathcal{V}_f. \end{aligned} \tag{2.5}$$

We let $R : \mathcal{V} \to \mathcal{V}'$ denote the residual defined by

$$(R(v), w) = (f, w) - a(v, w) \quad \text{for all } w \in \mathcal{V}. \tag{2.6}$$

The fine scale equation now takes the form: find $u_f \in \mathcal{V}_f$ such that

$$a(u_f, v_f) = (R(u_c), v_f) \quad \text{for all } v_f \in \mathcal{V}_f. \tag{2.7}$$

Thus the fine scale solution is driven by the residual of the coarse scale solution. Denoting the solution u_f to (2.7) by $u_f = \mathcal{T}R(u_c)$ we get the modified coarse scale problem

$$a(u_c, v_c) + a(\mathcal{T}R(u_c), v_c) = (f, v_c) \quad \text{for all } v_c \in \mathcal{V}_c. \tag{2.8}$$

Here the second term on the left hand side accounts for the effects of fine scales on the coarse scales.

In terms of matrices this gives us a modified stiffness matrix and a modified right hand side since $a(\mathcal{T}R(\phi_i), \phi_j) = T_{ij} + d_j$ for some matrix T and vector d. Note that $(R(v), w)$ defined in equation (2.6) is affine in v. If we denote the standard Galerkin stiffness matrix by A and the right hand side by b we would get $AU_G = b$ for the standard Galerkin but

$$(A + T)U_c = b - d, \tag{2.9}$$

for the modified version.

Another approach is to solve equation (2.5) iteratively with the Galerkin solution as an initial guess.

2.3 Approximation of Fine Scale Equations Based on Localized Dirichlet Problems

We use the method described in our earlier work [10, 11] for the approximate solution of the fine scale equations. The idea is to decouple the fine scale equations by including a partition of unity in the right hand side and then to solve the resulting problems on patches. We start with some preliminary notations.

We introduce a partition $\mathcal{K} = \{K\}$ of the domain Ω into coarse shape regular elements K of diameter H_K and we let $\mathcal{N}$ be the set of coarse nodes. Further we let $\mathcal{V}_c$ be the space of continuous piecewise polynomials of degree p defined on $\mathcal{K}$.

We let $u_f = \sum_{i \in \mathcal{N}} u_{f,i}$ where

$$a(u_{f,i}, v_f) = (\varphi_i R(u_c), v_f) \quad \text{for all } v_f \in \mathcal{V}_f, \tag{2.10}$$

and $\{\varphi_i\}_{i \in \mathcal{N}}$ is a partition of unity e. g. the set of Lagrange basis functions in $\mathcal{V}_c$, be the solution to the decoupled fine scale equations. We note that the right hand side has the same support as φ_i and a small support compared to Ω.

We introduce this expansion of u_f in the right hand side of the fine scale equation (2.5) and get: find $u_c \in \mathcal{V}_c$ and $u_f = \sum_{i \in \mathcal{N}} u_{f,i} \in \mathcal{V}_f$ such that

$$\begin{aligned} a(u_c, v_c) + a(u_f, v_c) = (f, v_c) \quad &\text{for all } v_c \in \mathcal{V}_c, \\ a(u_{f,i}, v_f) = (\varphi_i R(u_c), v_f) \quad &\text{for all } v_f \in \mathcal{V}_f \text{ and } i \in \mathcal{N}. \end{aligned} \tag{2.11}$$

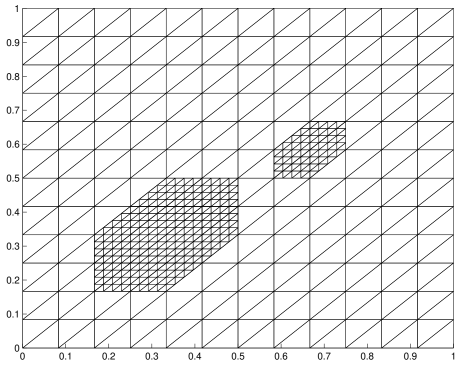

Figure 1: Two (left) and one (right) layer stars.

The next step is to solve the fine scale equations approximately. For each element in the partition of unity we associate a domain ω_i on which we solve Dirichlet problems. The local domain ω_i contains the support of the element in the partition of unity and is large enough to give a good approximate solution. The quality of the solution is controlled by error estimates. We now define the local finite element space $\mathcal{V}_f^h(\omega_i)$ associated with node i. We refine the coarse mesh on the patch ω_i and let $\mathcal{V}_f^h(\omega_i)$ be the fine part of the hierarchical basis on this mesh. Figure 1 shows patches and the mesh.

The resulting method reads: find $U_c \in \mathcal{V}_c$ and $U_f = \sum_i^n U_{f,i}$ where $U_{f,i} \in \mathcal{V}_f^h(\omega_i)$ such that

$$\begin{aligned} a(U_c, v_c) + a(U_f, v_c) &= (f, v_c) \quad \text{for all } v_c \in \mathcal{V}_c, \\ a(U_{f,i}, v_f) &= (\varphi_i R(U_c), v_f) \quad \text{for all } v_f \in \mathcal{V}_f^h(\omega_i) \text{ and } i \in \mathcal{N}. \end{aligned} \tag{2.12}$$

Since the functions in the local finite element spaces $\mathcal{V}_f^h(\omega_i)$ are equal to zero on $\partial\omega_i$, U_f and therefore U will be continuous.

Remark 2.1 For problems with multiscale phenomena on a part of the domain it is not necessary to solve local problems for all coarse nodes. We let $\mathcal{C} \subset \mathcal{N}$ refer to nodes where no local problems are solved and $\mathcal{F} \subset \mathcal{N}$ refer to nodes where local problems are solved. Obviously $\mathcal{C} \cup \mathcal{F} = \mathcal{N}$. We let $U_{f,i} = 0$ for $i \in \mathcal{C}$.

Remark 2.2 The choice of the subdomains ω_i is crucial for the method. We introduce a notation for mesh stars of many layers of coarse elements recursively in the following way. Let S_i^1 be the support of the coarse scale Lagrangian base function in node i. The extended mesh star $S_L^i = \cup_{j \in S_{L-1}^i} S_1^j$ for $L > 1$. We refer to L as the numbers of layers, see Figure 1.

To get an idea of how the localized solution $U_{f,i}$ behaves when the domain ω_i increases we plot different solutions $U_{f,i}$ in a smooth region of the solution u in Figure 2. Since $U_{f,i}$ is solved in the slice space $\mathcal{V}_f$ and since the right hand side of the fine scale equations of (2.12) has the same support as φ_i, $U_{f,i}$ will decay rapidly towards the boundary of ω_i, this

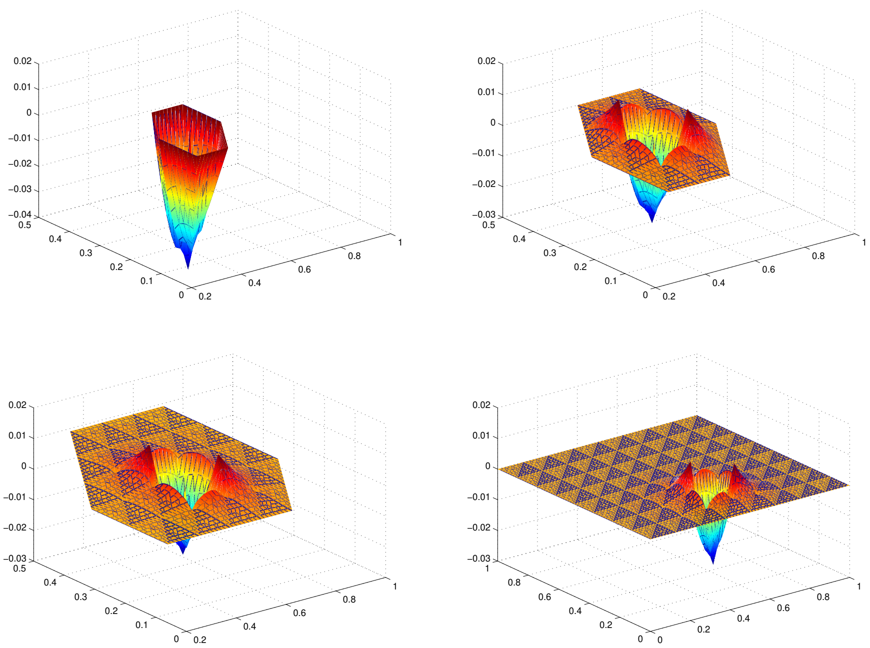

Figure 2: A typical localized solution $U_{f,i}$ of the fine scale equations in a smooth region using one, two, three layer stars, and the entire domain.

can also be seen in Figure 2. We can see that one layer stars appears to give bad accuracy while two and more layer stars captures the features of the correct solution.

3 A Posteriori Error Estimate in the Energy Norm

We start by introducing notations for bounds of the residual. Let $\mathcal{R}(U)$ be a bound of the residual defined in the following way, see [5]:

$$\mathcal{R}(U) = |f + \nabla \cdot a\nabla U| + \frac{1}{2} \max_{\partial K \setminus \Gamma} h_K^{-1} |[a\partial_n U]| \quad \text{on } K \in \mathcal{K}, \tag{3.1}$$

where $\mathcal{K}$ is the set of elements in the mesh and $[\cdot]$ is the difference in function value over the current interior edge. We note that $|(R(U), v)| \leq \|h^s \mathcal{R}(U)\| \|h^{-s} v\|$ for $s \in \mathbf{R}$. We define $\mathcal{R}_i(U_{f,i})$ in the same way as $\mathcal{R}(U)$ on the local mesh but with U replaced by $U_{f,i}$ and f replaced by $\varphi_i \mathcal{R}(U_c)$.

We also define a new space on the patches ω_i. Let $\mathcal{V}_f^h(\bar{\omega}_i)$ be the space of piecewise polynomials of degree p defined on the mesh on ω_i. This space is identical to $\mathcal{V}_f^h(\omega_i)$ with the difference that $\mathcal{V}_f^h(\bar{\omega}_i)$ is not necessarily zero on the boundary $\partial\omega_i$. This means that $\mathcal{V}_f^h(\omega_i) \subset \mathcal{V}_f^h(\bar{\omega}_i)$.

We derive an error estimate involving both the coarse scale error $e_c = u_c - U_c$ and the fine scale error $e_f = \sum_{i\in\mathcal{N}} e_{f,i} := \sum_{i\in\mathcal{N}} (u_{f,i} - U_{f,i})$ that arises from using our finite element method (2.12).

If we subtract the coarse part of equation (2.12) from the coarse part of equation (2.11) we get the Galerkin orthogonality,

$$a(e_c, v_c) + a(e_f, v_c) = 0 \quad \text{for all } v_c \in \mathcal{V}_c. \tag{3.2}$$

The same argument on the fine scale equation gives for $i \in \mathcal{F}$,

$$a(e_{f,i}, v_f) = (f, \varphi_i v_f) - a(e_c, \varphi_i v_f), \quad \text{for all } v_f \in \mathcal{V}_f^h(\omega_i). \tag{3.3}$$

We state the following estimate for the error in the energy norm, $\|e\|_a = a(e,e)^{1/2}$.

Theorem 3.1 *It holds,*

$$\begin{aligned} \|e\|_a^2 \leq{}& C \sum_{i\in\mathcal{C}} \|H\mathcal{R}(U_c)\|_{\omega_i}^2 \|\frac{1}{\sqrt{a}}\|_{L^\infty(\omega_i)}^2 \\ &+ C \sum_{i\in\mathcal{F}} \left(\|\sqrt{H}\Sigma(U_{f,i})\|_{\partial\omega_i}^2 + \|h\mathcal{R}_i(U_{f,i})\|_{\omega_i}^2 \right) \|\frac{1}{\sqrt{a}}\|_{L^\infty(\omega_i)}^2, \end{aligned} \tag{3.4}$$

where

$$(-\Sigma(U_{f,i}), v_f)_{\partial\omega_i} = (\varphi_i R(U_c), v_f)_{\omega_i} - a(U_{f,i}, v_f)_{\omega_i}, \quad \textit{for all } v_f \in V_f^h(\bar{\omega}_i). \tag{3.5}$$

Proof. We use the error equation (3.2) with v_c as the Scott-Zhang interpolant $\pi_c e$ onto the coarse space $\mathcal{V}_c$, see [2], to get,

$$\begin{aligned}
\|e\|_a^2 &= a(e,e) && (3.6)\\
&= a(e, e-\pi_c e) && (3.7)\\
&= a(u-U_c, e-\pi_c e) - a(U_f, e-\pi_c e) && (3.8)\\
&= (R(U_c), e-\pi_c e) - a(U_f, e-\pi_c e) && (3.9)\\
&= \sum_{i\in\mathcal{C}} (\varphi_i R(U_c), e-\pi_c e) && (3.10)\\
&\quad + \sum_{i\in\mathcal{F}} (\varphi_i R(U_c), e-\pi_c e) - a(U_{f,i}, e-\pi_c e)\\
&= \sum_{i\in\mathcal{C}} (\varphi_i R(U_c), e-\pi_c e) && (3.11)\\
&\quad + \sum_{i\in\mathcal{F}} (\varphi_i R(U_c), \pi_{f,i}(e-\pi_c e)) - a(U_{f,i}, \pi_{f,i}(e-\pi_c e))\\
&\quad + \sum_{i\in\mathcal{F}} (\varphi_i R(U_c), e-\pi_c e - \pi_{f,i}(e-\pi_c e))\\
&\qquad - \sum_{i\in\mathcal{F}} a(U_{f,i}, e-\pi_c e - \pi_{f,i}(e-\pi_c e))\\
&= \mathrm{I} + \mathrm{II} + \mathrm{III} && (3.12)
\end{aligned}$$

where $\pi_{f,i}$ is the Scott-Zhang interpolant onto $\mathcal{V}_f^h(\bar{\omega}_i)$. We start by estimating the first term of equation (3.12), I. From interpolation theory [2] we have,

$$\begin{aligned}
\sum_{i\in\mathcal{C}} (\varphi_i R(U_c), e-\pi_c e) &\le \sum_{i\in\mathcal{C}} \|\varphi_i R(U_c)\|_{\omega_i} \|e-\pi_c e\|_{\omega_i} && (3.13)\\
&\le C \sum_{i\in\mathcal{C}} \|H\mathcal{R}(U_c)\|_{\omega_i} \|\nabla e\|_{\omega_i}. && (3.14)
\end{aligned}$$

Next we turn our attention to the second term of equation (3.12), II. We introduce $\Sigma(U_{f,i})$ as the piecewise polynomial defined on $\partial\omega_i$ that uniquely solves,

$$(-\Sigma(U_{f,i}), v_f)_{\partial\omega_i} = (R(U_c), \varphi_i v_f)_{\omega_i} - a(U_{f,i}, v_f)_{\omega_i}, \quad \text{for all } v_f \in V_f^h(\bar{\omega}_i). \tag{3.15}$$

With this definition we get the following estimate for the second term,

$$\begin{aligned}
\mathrm{II} &= \sum_{i\in\mathcal{F}} (-\Sigma(U_{f,i}), \pi_{f,i}(e-\pi_c e))_{\partial\omega_i} && (3.16)\\
&\le \sum_{i\in\mathcal{F}} \|\sqrt{H}\Sigma(U_{f,i})\|_{\partial\omega_i} \|\frac{1}{\sqrt{H}} \pi_{f,i}(e-\pi_c e)\|_{\partial\omega_i}. && (3.17)
\end{aligned}$$

We use the the following trace inequality from [2],

$$\|\pi_{f,i}(e-\pi_c e)\|_{\partial\omega_i}^2 \leq C\left(\frac{1}{H}\|\pi_{f,i}(e-\pi_c e)\|_{\omega_i}^2 + H\|\nabla\pi_{f,i}(e-\pi_c e)\|_{\omega_i}^2\right). \tag{3.18}$$

Next we use that the Scott-Zhang interpolant is both L^2 and H^1 stable on shape-regular meshes from [4, 3] to get,

$$\begin{aligned}\|\pi_{f,i}(e-\pi_c e)\|_{\partial\omega_i}^2 &\leq C\left(\frac{1}{H}\|e-\pi_c e\|_{\omega_i}^2 + H\|\nabla(e-\pi_c e)\|_{\omega_i}^2\right) &(3.19)\\ &\leq CH\|\nabla e\|_{\omega_i}^2. &(3.20)\end{aligned}$$

We conclude

$$\mathrm{II} \leq C\sum_{i\in\mathcal{F}}\|\sqrt{H}\Sigma(U_{f,i})\|_{\partial\omega_i}\|\nabla e\|_{\omega_i}. \tag{3.21}$$

We now take on the third term in equation (3.12), $\sum_{i\in\mathcal{F}}(\varphi_i R(U_c), e-\pi_c e-\pi_{f,i}(e-\pi_c e)) - a(U_{f,i}, e-\pi_c e-\pi_{f,i}(e-\pi_c e))$,

$$\begin{aligned}\mathrm{III} &\leq C\sum_{i\in\mathcal{F}}\|h\mathcal{R}_i(U_{f,i})\|_{\omega_i}\|\nabla(e-\pi_c e)\|_{\omega_i} &(3.22)\\ &\leq C\sum_{i\in\mathcal{F}}\|h\mathcal{R}_i(U_{f,i})\|_{\omega_i}\|\nabla e\|_{\omega_i}. &(3.23)\end{aligned}$$

We need to do the following simple observation,

$$\|\nabla e\|_{\omega_i} \leq \|\frac{1}{\sqrt{a}}\|_{L^\infty(\omega_i)}\|\sqrt{a}\nabla e\|_{\omega_i}, \tag{3.24}$$

by Hölder's inequality. We go back to equation (3.6) and use the estimates of the three terms together with equation (3.24)

$$\begin{aligned}\|e\|_a^2 \le &\sum_{i\in\mathcal{C}}(\varphi_i R(U_c), e-\pi_c e) \\ &+\sum_{i\in\mathcal{F}}(\varphi_i R(U_c), \pi_{f,i}(e-\pi_c e)) - a(U_{f,i}, \pi_{f,i}(e-\pi_c e)) \\ &+\sum_{i\in\mathcal{F}}(\varphi_i R(U_c), e-\pi_c e-\pi_{f,i}(e-\pi_c e)) \\ &-\sum_{i\in\mathcal{F}} a(U_{f,i}, e-\pi_c e-\pi_{f,i}(e-\pi_c e))\end{aligned} \tag{3.25}$$

$$\begin{aligned}\le\ & C\sum_{i\in\mathcal{C}}\|H\mathcal{R}(U_c)\|_{\omega_i}\|\nabla e\|_{\omega_i} \\ &+C\sum_{i\in\mathcal{F}}\|\sqrt{H}\Sigma(U_{f,i})\|_{\partial\omega_i}\|\nabla e\|_{\omega_i} \\ &+C\sum_{i\in\mathcal{F}}\|h\mathcal{R}_i(U_{f,i})\|_{\omega_i}\|\nabla e\|_{\omega_i}\end{aligned} \tag{3.26}$$

$$\begin{aligned}\le\ & C\left(\sum_{i\in\mathcal{C}}\|H\mathcal{R}(U_c)\|_{\omega_i}^2\|\frac{1}{\sqrt{a}}\|^2_{L^\infty(\omega_i)}\right)^{1/2}\|e\|_a \\ &+C\left(\sum_{i\in\mathcal{F}}\|\sqrt{H}\Sigma(U_{f,i})\|_{\partial\omega_i}^2\|\frac{1}{\sqrt{a}}\|^2_{L^\infty(\omega_i)}\right)^{1/2}\|e\|_a \\ &+C\left(\sum_{i\in\mathcal{F}}\|h\mathcal{R}_i(U_{f,i})\|_{\omega_i}^2\|\frac{1}{\sqrt{a}}\|^2_{L^\infty(\omega_i)}\right)^{1/2}\|e\|_a\end{aligned} \tag{3.27}$$

Finally we get

$$\begin{aligned}\|e\|_a^2 \le &\ C\sum_{i\in\mathcal{C}}\|H\mathcal{R}(U_c)\|_{\omega_i}^2\|\frac{1}{\sqrt{a}}\|^2_{L^\infty(\omega_i)} \\ &+C\sum_{i\in\mathcal{F}}\left(\|\sqrt{H}\Sigma(U_{f,i})\|_{\partial\omega_i}^2+\|h\mathcal{R}_i(U_{f,i})\|_{\omega_i}^2\right)\|\frac{1}{\sqrt{a}}\|^2_{L^\infty(\omega_i)},\end{aligned} \tag{3.28}$$

which proves the theorem. □

Remark 3.1 We need to motivate the definition of $\Sigma(U_{f,i})$:

$$(-\Sigma(U_{f,i}), v_f)_{\partial\omega_i} = (\varphi_i R(U_c), v_f)_{\omega_i} - (a\nabla U_{f,i}, \nabla v_f)_{\omega_i}, \quad \text{for all } v_f \in \mathcal{V}_f^h(\bar{\omega}_i), \tag{3.29}$$

in equation (3.5). The function $\Sigma(U_{f,i})$ is a piecewise polynomial defined on the boundary of patch ω_i. Remember that

$$(\varphi_i R(U_c), v_f)_{\omega_i} - (a\nabla U_{f,i}, \nabla v_f)_{\omega_i} = 0, \quad \text{for all } v_f \in \mathcal{V}_f^h(\omega_i), \tag{3.30}$$

This means that have the same number of unknowns and equations and in practice calculating $\Sigma(U_{f,i})$ will come down to solving a linear system with a mass matrix defined on the boundary of the patch. The function $\Sigma(U_{f,i})$ is a variational approximation of $n \cdot a\nabla U_{f,i}$. This is further discussed in [8].

4 Periodic Coefficient

Many multiscale applications features periodic fine scale structure. In this special case we can get more information out of our calculations. We assume that we have local scale of size ϵ and a global scale of size 1. Further we assume $a = a(x/\epsilon)$ to be smooth. If we discretize Poisson's equation with a mesh parameter $H > \epsilon$ using the standard Galerkin finite element method we have the following estimate from [6].

Proposition 4.1 *It holds*

$$\|e\|_a \leq C\frac{H}{\epsilon}\|f\|. \tag{4.1}$$

Here $f \in L^2(\Omega)$. From this estimate it is clear that we can not hope to get a good approximation without resolving the fine scales. If we make a similar calculation for the variational multiscale approach presented in this paper we get the following.

Theorem 4.1 *It holds*

$$\|e\|_a^2 \leq C\left(\frac{h}{\epsilon}\right)^2\|f\|^2 + C\sum_{K\in\mathcal{K}}\|\sqrt{H}\Sigma(U_{f,i})\|_{\partial\omega_i}^2\|\frac{1}{\sqrt{a}}\|_{L^\infty(\omega_i)}^2. \tag{4.2}$$

Proof. We use a global Scott-Zhang interpolant of v on the fine mesh associated with h, πv, in the following calculation,

$$\begin{aligned}
\|e\|_a^2 &= a(e,e) && (4.3)\\
&= a(e, e-\pi e) + a(e, \pi(e-\pi_c e)) && (4.4)\\
&= a(e, u_f - \pi u_f) + \sum_{i\in\mathcal{N}} a(e_c, \varphi_i\pi_{f,i}(e-e_c)) + a(e_{f,i}, \pi(e-\pi_c e)) && (4.5)\\
&= a(e, u_f - \pi u_f) + \sum_{i\in\mathcal{N}}(\Sigma(U_{f,i}), \pi_{f,i}(e-\pi_c e))_{\partial\omega_i} && (4.6)\\
&= \mathrm{I} + \mathrm{II}. && (4.7)
\end{aligned}$$

The first part, I in equation (4.3), is standard and can be estimated as follows,

$$I \leq \frac{1}{4}\|e\|_a^2 + \|u_f - \pi u_f\|_a^2 \leq \frac{1}{4}\|e\|_a^2 + C\left(\frac{h}{\epsilon}\right)^2\|f\|^2. \tag{4.8}$$

For the second part, II in equation (4.3), we use Cauchy-Schwarz for sums, the H^1-stability of π, see [4, 3], and $u_f = u - u_c$ to get,

$$II \leq \sum_{i\in\mathcal{N}} \sqrt{H}\|\Sigma U_{f,i}\|_{\partial\omega_i}\|\frac{1}{\sqrt{H}}\pi_{f,i}(e-\pi_c e)\|_{\omega_i} \tag{4.9}$$

$$\leq \sum_{i\in\mathcal{N}} \sqrt{H}\|\Sigma U_{f,i}\|_{\partial\omega_i}\|\frac{1}{\sqrt{H}}\pi_{f,i}(e-\pi_c e)\|_{\omega_i}. \tag{4.10}$$

We use Cauchy-Schwarz for sums, equation (3.20), and (3.24) to get,

$$II \leq C\left(\sum_{i\in\mathcal{N}} \|\sqrt{H}\Sigma U_{f,i}\|^2\|\frac{1}{\sqrt{a}}\|^2_{L^\infty(\omega_i)}\right)^{1/2} \|e\|_a \tag{4.11}$$

$$\leq C\sum_{i\in\mathcal{N}} \|\sqrt{H}\Sigma U_{f,i}\|^2\|\frac{1}{\sqrt{a}}\|^2_{L^\infty(\omega_i)} + \frac{1}{4}\|e\|_a^2. \tag{4.12}$$

We combine equation (4.7), (4.8), and (4.12) to prove the theorem. □

When solving problems with periodic coefficients it is very reasonable to choose structured meshes if possible aligned with the oscillations. It is also natural to put in equal computational effort in all parts of the domain which means that no adaptivity in terms of where the fine scale should be solved is necessary. However, it is still important to choose the relation between the parameters h and L adaptively.

If the mesh is aligned with the oscillations local problems solved inside the domain will differ only in the right hand side which means that the computational effort is almost nothing. If f is also periodic we would get identical contributions to the modifying matrix T in equation (2.9) from the local calculations.

Patches including parts of the boundary will also appear repeatedly in the calculations.

5 Adaptive Algorithm

We use the energy norm estimate in Theorem 3.1 to construct an adaptive algorithm. Recall the result,

$$\begin{aligned}\|e\|_a^2 \leq{}& C\sum_{i\in\mathcal{C}} \|H\mathcal{R}(U_c)\|^2_{\omega_i}\|\frac{1}{\sqrt{a}}\|^2_{L^\infty(\omega_i)} \\ &+ C\sum_{i\in\mathcal{F}}\left(\|\sqrt{H}\Sigma(U_{f,i})\|^2_{\partial\omega_i} + \|h\mathcal{R}_i(U_{f,i})\|^2_{\omega_i}\right)\|\frac{1}{\sqrt{a}}\|^2_{L^\infty(\omega_i)},\end{aligned} \tag{5.1}$$

These contributions to the error can easily be understood. The first term is the standard a posteriori error estimate for a Galerkin solution on the coarse mesh i.e. this is what we get if we do not solve any local problems. The first part of the second sum represents the

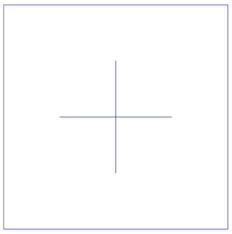

Figure 3: Unit square with slits between $(0.25, 0.5)$ and $(0.75, 0.5)$ and between $(0.5, 0.25)$ and $(0.5, 0.75)$.

error arising from the fact that we solve the local problems on patches ω_i instead of the whole domain. Remember that $\Sigma(U_{f,i})$ is closely related to the normal derivative of the fine scale solution on the boundary of the patches. Finally, the second part of the second sum represents the fine scale resolution. The two contributions to the second sum clearly points out the parameters of interest when using our method. The first one is the patch size, increasing patch size will decrease $\|\sqrt{H}\Sigma_i(U_{f,i})\|_{\partial\omega_i}$, the second one is the fine scale mesh size h.

From equation (5.1) we now state the following adaptive algorithm:

Adaptive Algorithm.

1. Start with no nodes in $\mathcal{F}$.
2. Calculate a solution U_c on the coarse mesh by solving (2.12).
3. For all $i \in \mathcal{C}$ calculate the residuals for each coarse node, $R_i = \|H\mathcal{R}(U_c)\|^2_{\omega_i}$.
4. For all $i \in \mathcal{F}$ calculate the contributions from the first term of the local problems, $S_i = \|\sqrt{H}\Sigma(U_{f,i})\|^2_{\partial\omega_i}$ and the second term, $W_i = \|h\mathcal{R}_i(U_{f,i})\|^2_{\omega_i}$.
5. For large values in R_i add i to $\mathcal{F}$, for large values in S_i or W_i either increase the number of layers or decrease the fine scale mesh size h for local problem i. Return to 2 or stop if the desired tolerance is reached.

6 Numerical Examples

We solve two dimensional model problems with linear base functions defined on a uniform triangular mesh.

Example 1. In the first example we let $a = 1$, $f = 1$, and Ω be the unit square with a crack that forms a plus sign, see Figure 3. The solution u is forced to be zero on the boundary including the slits, see Figure 4. We solve the problem by using the adaptive

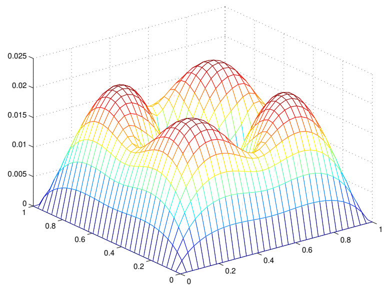

Figure 4: The solution calculated using 1089 nodes.

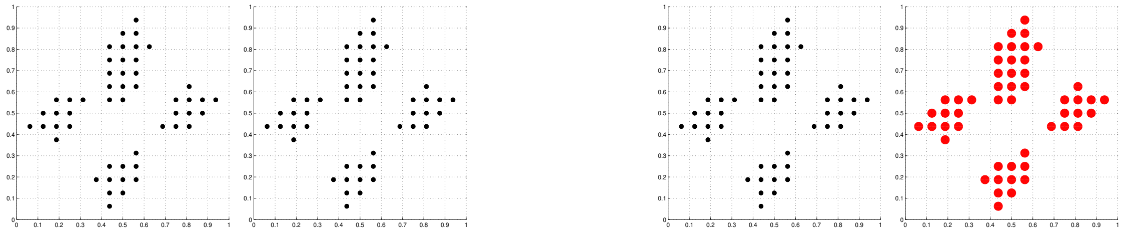

Figure 5: Refinement level, $h = H \cdot 2^{-k}$, and number of layers L for each coarse node after the first (left) and second (right) iteration. We have $k = 1$ and $L = 1$ (left) and $L = 2$ (right).

algorithm above with a refinement level of 8 % in each iteration. We start with one refinement and one layer stars for the local problems. Figure 5 (left) shown the adaptive choice of coarse nodes for which local problems needs to be solved.

After the second iteration no more local problems are added but the number of layers is increased to two, see Figure 5 (right). As seen the algorithm decides to increase the number of layers for all coarse nodes. This indicates that the normal derivative of $U_{f,i}$ is not small on the boundary of the patches. This is exactly what we get if we study a specific choice of $U_{f,i}$ with center close to the cracks, see Figure 6. These solutions looks quite different from the ones that origins from a smooth region found in Figure 2. The local contribution has a constant sign which indicates a constant signed error in the Galerkin solution. In Figure 7 we study the error compared to a reference solution of the standard Galerkin solution and the solutions after one and two iterations. The Galerkin solution has large errors in the singularities and that the error is positive. We see that the local problems decreases the error in each iteration.

Example 2. In this example we use a simple geometry, the unit square, but we let the coefficient a oscillate rapidly according to Figure 8. We calculate a reference solution on the fine space and compare it to standard Galerkin calculated using quadrature on the coarse mesh with and without solving local problems. We see that standard Galerkin on

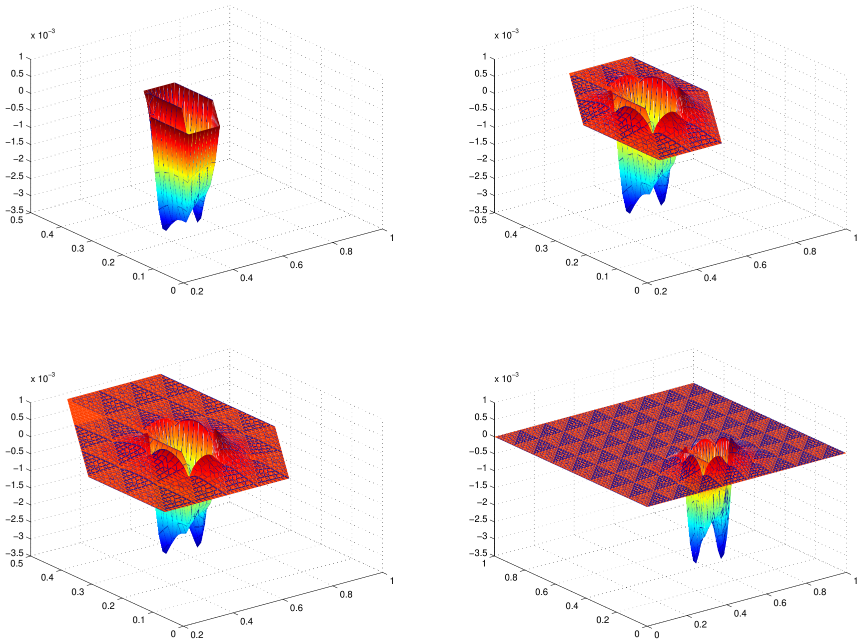

Figure 6: Localized solution $U_{f,i}$ to the fine scale equations in a rough region using one, two, three layer stars, and the entire domain.

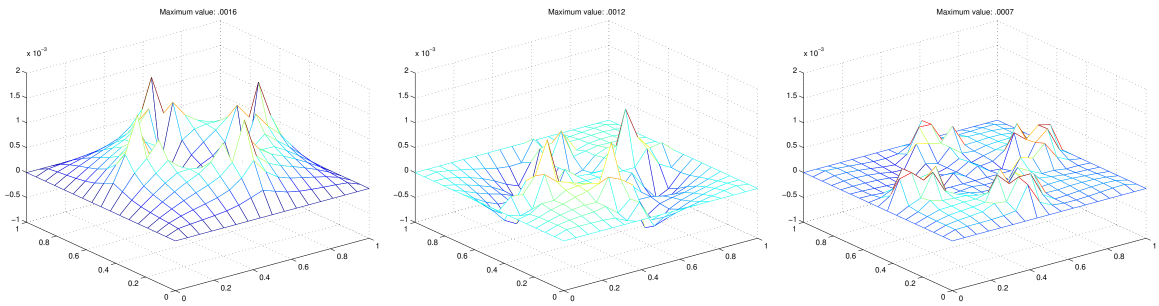

Figure 7: The error in the Galerkin solution (left), after one step in the adaptive algorithm (middle), and after two steps (right).

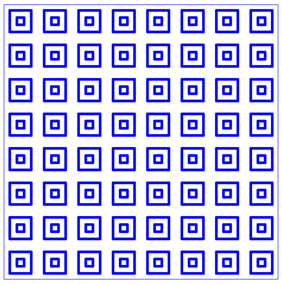

Figure 8: The coefficient is discontinuous with the values $a = 1$ on the white areas and $a = 0.05$ on the dark areas.

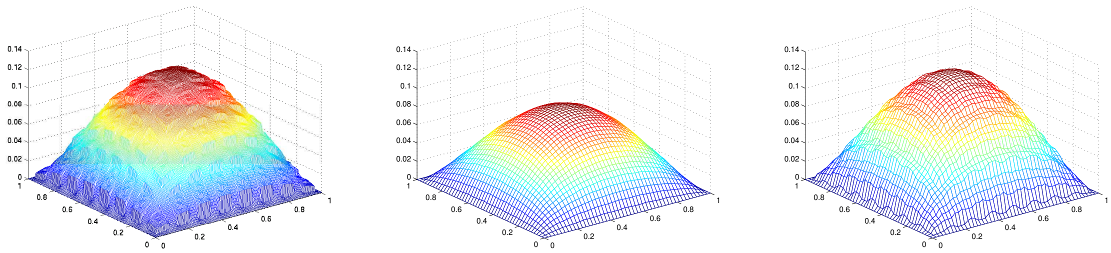

Figure 9: Reference solution (left), standard Galerkin on coarse mesh (middle), and solution with local problems using two layer stars (right).

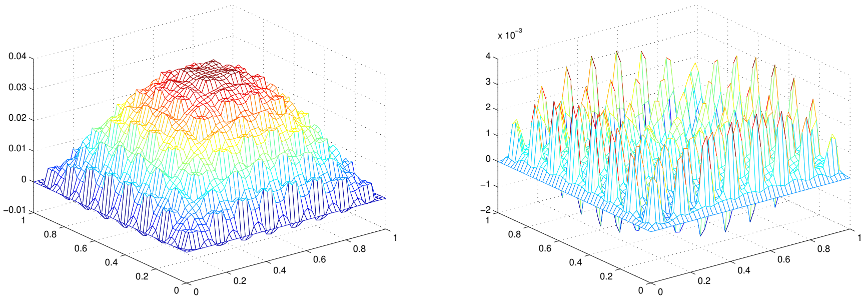

Figure 10: Error for standard Galerkin (left) and for the solution with local problems using two layer stars (right).

a coarse mesh performs badly for this problem, Figure 9. This is not surprising. From equation (4.1) we see that we have no control of the error what so ever when using Galerkin on a coarse mesh. The solution calculated using two layer stars other hand gives a very nice improvement of the solution. The magnitude is now correct and if we study the error between this solution and the reference solution we get a ten times smaller error, see Figure 10. The coarse mesh is aligned to the oscillations in a so this nice solution can be calculated by solving extremely few small localized problems to very low cost.

As mentioned before calculating a modified stiffness matrix rather than using an iterative approach is very efficient in the periodic setting. To understand the method it is interesting to know how the method actually modifies the stiffness matrix. We do this by studying the spectrum of the resulting matrix $A+T$ for different number of layers in Figure 11. We study the twenty lowest and most significant eigenvalues. The first thing we note is that the eigenvalues of $A+T$ always is smaller than the ones of A. This is natural since the discretization increases eigenvalues of the operator. We also see that already after two layers we get very nice agreement with the correct spectrum we like to approximate.

Our experience form using this method is that one layer stars almost never is enough to get good accuracy but already two layer stars gives very nice improvement of the Galerkin solution.

References

[1] T. Arbogast and S. L. Bryant, A two-scale numerical subgrid technique for waterflood simulations, SPE J., Dec. 2002, pp 446-457.

[2] S. C. Brenner and L. R. Scott, *The mathematical theory of finite element methods,* Springer Verlag, 1994.

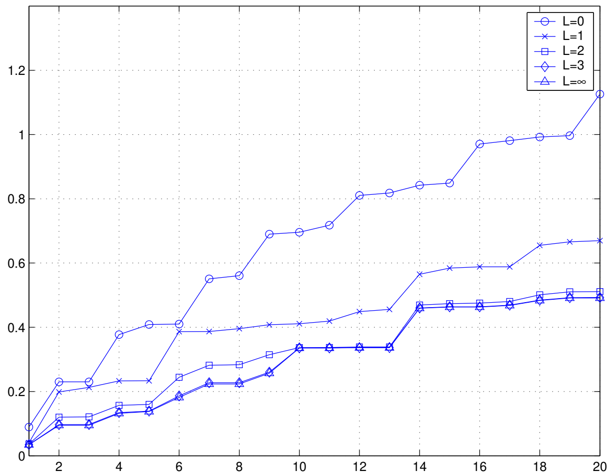

Figure 11: The twenty lowest eigenvalues of the matrix $A+T$ for fine scale problems solved using no stars, one layer stars, two layer stars, three layer stars, and the entire domain.

[3] C. Carstensen, *Merging the Bramble-Pasciak-Steinbach and the Crouzeix-Thomée criterion for the H^1-stability of the L^2-projection onto finite element spaces,* Math. Comp., 71, 237, 157-163, 2002.

[4] M. Crouzeix and V. Thomée, *The Stability in L_p and W_p^1 of the L_2-projection onto Finite Element Function Spaces,* Mathematics of Computation, 48, 178, 521-532, 1987.

[5] K. Eriksson, D. Estep, P. Hansbo and C. Johnson, *Computational differential equations,* Studentlitteratur, 1996.

[6] T. Y. Hou and X.-H. Wu, *A multiscale finite element method for elliptic problems in composite materials and porous media,* J. Comput. Phys. 134 (1997) 169-189.

[7] T. J.R. Hughes, *Multiscale phenomena: Green's functions, the Dirichlet-to-Neumann formulation, subgrid scale models, bubbles and the origins of stabilized methods,* Comput. Methods Appl. Mech. Engrg. 127 (1995) 387-401.

[8] T. J.R. Hughes, L Mazzei, A. A. Oberai, and M. G. Larson, *The continuous Galerkin method is locally conservative,* J. Comput. Phys., Vol. 163(2) (2000) 467-488.

[9] T. J.R. Hughes, G. R. Feijóo, L. Mazzei and Jean-Baptiste Quincy, *The variational multiscale method - a paradigm for computational mechanics,* Comput. Methods Appl. Mech. Engrg. 166 (1998) 3-24.

[10] M. G. Larson and A. Målqvist, *Adaptive variational multiscale methods based on a posteriori error estimation: Duality techniques for elliptic problmes,* to appear in Proceedings of the workshop Multiscale Methods in Science and Engineering, Springer Verlag.

[11] M. G. Larson and A. Målqvist, *Adaptive variational multiscale methods based on a posteriori error estimation,* Proceedings of ECCOMAS 2004 conference, 2004.

[12] A. A. Oberai and P. M. Pinsky, *A multiscale finite element method for the Helmholtz equation,* Comput. Methods Appl. Mech. Engrg. 154 (1998) 281-297.

Chalmers Finite Element Center Preprints

2003–01	*A hybrid method for elastic waves* Larisa Beilina
2003–02	*Application of the local nonobtuse tetrahedral refinement techniques near Fichera-like corners* L. Beilina, S. Korotov and M. Křížek
2003–03	*Nitsche's method for coupling non-matching meshes in fluid-structure vibration problems* Peter Hansbo and Joakim Hermansson
2003–04	*Crouzeix–Raviart and Raviart–Thomas elements for acoustic fluid–structure interaction* Joakim Hermansson
2003–05	*Smoothing properties and approximation of time derivatives in multistep backward difference methods for linear parabolic equations* Yubin Yan
2003–06	*Postprocessing the finite element method for semilinear parabolic problems* Yubin Yan
2003–07	*The finite element method for a linear stochastic parabolic partial differential equation driven by additive noise* Yubin Yan
2003–08	*A finite element method for a nonlinear stochastic parabolic equation* Yubin Yan
2003–09	*A finite element method for the simulation of strong and weak discontinuities in elasticity* Anita Hansbo and Peter Hansbo
2003–10	*Generalized Green's functions and the effective domain of influence* Donald Estep, Michael Holst, and Mats G. Larson
2003–11	*Adaptive finite element/difference method for inverse elastic scattering waves* Larisa Beilina
2003–12	*A Lagrange multiplier method for the finite element solution of elliptic domain decomposition problems using non-matching meshes* Peter Hansbo, Carlo Lovadina, Ilaria Perugia, and Giancarlo Sangalli
2003–13	*A reduced P^1–discontinuous Galerkin method* R. Becker, E. Burman, P. Hansbo, and M.G. Larson
2003–14	*Nitsche's method combined with space–time finite elements for ALE fluid–structure interaction problems* Peter Hansbo, Joakim Hermansson, and Thomas Svedberg
2003–15	*Stabilized Crouzeix–Raviart element for the Darcy-Stokes problem* Erik Burman and Peter Hansbo

2003–16 *Edge stabilization for the generalized Stokes problem: a continuous interior penalty method*
Erik Burman and Peter Hansbo

2003–17 *A conservative flux for the continuous Galerkin method based on discontinuous enrichment*
Mats G. Larson and A. Jonas Niklasson

2003–18 *CAD–to–CAE integration through automated model simplification and adaptive modelling*
K.Y. Lee, M.A. Price, C.G. Armstrong, M.G. Larson, and K. Samuelsson

2003–19 *Multi-adaptive time integration*
Anders Logg

2003–20 *Adaptive computational methods for parabolic problems*
Kenneth Eriksson, Claes Johnson, and Anders Logg

2003–21 *The FEniCS project*
T. Dupont, J. Hoffman, C. Johnson, R.C. Kirby, M.G. Larson, A. Logg, and R. Scott

2003–22 *Adaptive finite element methods for LES: Computation of the mean drag coefficient in a turbulent flow around a surface mounted cube using adaptive mesh refinement*
Johan Hoffman

2003–23 *Adaptive DNS/LES: a new agenda in CFD*
Johan Hoffman and Claes Johnson

2003–24 *Multiscale convergence and reiterated homogenization of parabolic problem*
Anders Holmbom, Nils Svanstedt, and Niklas Wellander

2003–25 *On the relationship between some weak compactnesses with different numbers of scales*
Anders Holmbom, Jeanette Silfver, Nils Svanstedt, and Niklas Wellander

2003–26 *A posteriori error estimation in computational inverse scattering*
Larisa Beilina and Claes Johnson

2004–01 *Computability and adaptivity in CFD*
Johan Hoffman och Claes Johnson

2004–02 *Interpolation estimates for piecewise smooth functions in one dimension*
Anders Logg

2004–03 *Estimates of derivatives and jumps across element boundaries for multi-adaptive Galerkin solutions of ODEs*
Anders Logg

2004–04 *Multi-adaptive Galerkin methods for ODEs III: Existence and stability*
Anders Logg

2004–05 *Multi-adaptive Galerkin methods for ODEs IV: A priori error estimates*
Anders Logg

2004–06 *A stabilized non-conforming finite element method for incompressible flow*
Erik Burman and Peter Hansbo

2004–07 *On the uniqueness of weak solutions of Navier-Stokes equations: Remarks on a Clay Institute prize problem*
Johan Hoffman and Claes Johnson

2004–08 *A new approach to computational turbulence modeling*
Johan Hoffman and Claes Johnson

2004–09 *A posteriori error analysis of the boundary penalty method*
Kenneth Eriksson, Mats G. Larson, and Axel Målqvist

2004–10 *A posteriori error analysis of stabilized finite element approximations of the helmholtz equation on unstructured grids*
Mats G. Larson and Axel Målqvist

2004–11 *Adaptive variational multiscale methods based on a posteriori error estimation*
Mats G. Larson and Axel Målqvist

2004–12 *Multi-adaptive Galerkin methods for ODEs V: Stiff problems*
Johan Jansson and Anders Logg

2004–13 *Algorithms for multi-adaptive time-stepping*
Johan Jansson and Anders Logg

2004–14 *Simulation of mechanical systems with individual time steps*
Johan Jansson and Anders Logg

2004–15 *Computational modeling of dynamical systems*
Johan Jansson, Claes Johnson, and Anders Logg

2004–16 *Adaptive variational multiscale methods based on a posteriori error estimation: Duality techniques for elliptic problems*
Mats G. Larson and Axel Målqvist

2004–17 *Ultraconvergence of an interpolated finite element method for some fourth-order elliptic problems*
Andrey B. Andreev and Milena R. Racheva

2004–18 *Adaptive variational multiscale methods based on a posteriori error estimation: energy norm estimates for elliptic problems*
Mats G. Larson and Axel Målqvist

These preprints can be obtained from

`www.phi.chalmers.se/preprints`